1.6 UPPER LIMIT OF THE X-RAY POLARIZATION OF THE CRAB NEBULA*

R. NOVICK, J. R. P. ANGEL and R. S. WOLFF
Columbia Astrophysics Laboratory, Columbia University, New York, N.Y. U.S.A.

Abstract. A rocket-borne X-ray polarimeter was flown to search for polarization in Taurus X-1. Although a result consistent with zero polarization was obtained, the statistics were such that X-ray polarization comparable in magnitude and direction to that of radio and optical continuum emission cannot be excluded.

1. Introduction

An X-ray polarimeter utilizing incoherent scattering was constructed and flown in an Aerobee-150 sounding rocket at 0327 UT on March 7, 1969, to search for polarization in the X-ray emission of Taurus X-1 (Wolff *et al.*, 1970). Four minutes of data obtained while the polarimeter was above 250000 ft and aimed at the source have been analyzed to obtain the Stokes parameters describing the magnitude and orientation of the polarization of the X-ray emission. The values obtained are $q = 7.26 \pm 9.5\%$ and $u = -5.0 \pm 9.3\%$, where u and q are the normalized Stokes parameters. The quoted uncertainties are 1σ standard deviations in these quantities. A number of systematic effects have been considered and found to be unimportant compared to these statistical uncertainties. Expressed in terms of polarization, magnitude P, and position angle θ, measured east from north, our results are $p = 8.8\%$ and $\theta = 163°$.

The existence of polarization in the optical emission of the Crab nebula was first discovered in 1953 (Vashakidze, 1954) and since has been extensively studied. The magnitude and orientation of the optical polarization varies considerably over the 6′ extent of the nebula, but integrating over the entire object leads to a net result of about 9.3%. The degree of polarization increases as the field of view is narrowed, and has been measured as 19% with 1′ aperture centered on the luminous central region of the nebula (Oort and Walraven, 1956). Polarization in the strong radio emission of the nebula at 9.55 mm was observed by Hobbs (1968) as 13.8%. Measurements with various antenna beam widths and at different wavelengths have been made, leading to a rather complete picture of the intensity and polarization of radiation emitted by the nebula over a broad energy range. As suggested by Shklovsky in 1953, the spectral behavior and polarization of the visible and radio emission can be explained as synchrotron radiation from a power-law distribution of electrons moving in a magnetic field. The observed spectrum and polarization of the optical

* This work was supported in part by the National Aeronautics and Space Administration under Grants NGR-33-008-102, NGR-33-008-012, NGR-33-008-125 and Contract NAS 8-24668, and in part by the Air Force Office of Scientific Research under Grant AFOSR-70-1945. It is Columbia Astrophysics Laboratory Contribution No. 33.

Davies and Smith (eds.), The Crab Nebula, 54–64. All Rights Reserved.

https://doi.org/10.1017/S0074180900007208 Published online by Cambridge University Press

and radio radiation confirm this hypothesis, and the Crab nebula is generally accepted as a synchrotron emitter in this energy range.

The X-ray flux, first observed in 1963, originates in the central portion of the nebula (Bowyer *et al.*, 1964) and is coincident with the region of highest optical luminosity and polarization (Oda *et al.*, 1967). The X-ray data appear to be a natural extension of the synchrotron spectrum (Woltjer, 1964), in which case the X-ray and optical radiation would have comparable polarization. Serious questions have been raised regarding the source and lifetimes of relativistic electrons energetic enough to emit synchrotron radiation at X-ray wavelengths, and Sartori and Morrison (1967) have proposed a hot plasma model as an alternate X-ray production mechanism. The measurements of the spectral behavior of the X-ray flux cannot be used to distinguish between the two models, but a measurement of the X-ray polarization could serve as a definitive means of resolving these questions.

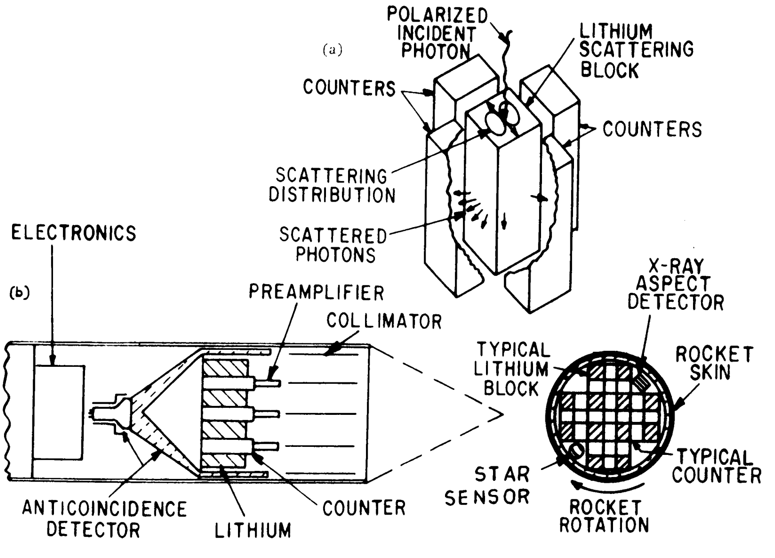

Fig. 1. (a) Schematic representation of the polarimeter concept. (b) Mounting of the polarimeter and ancillary equipment in the rocket.

The instrument used in the present work exploits the polarization dependence of Thomson scattering. The probability of scattering at an angle α to the electric vector of the incident radiation is proportional to $\sin^2\alpha$. Metallic lithium scattering blocks are used, with 3-atm xenon-methane proportional counters arranged to detect the radiation scattered out through the sides of the blocks. This is shown schematically in Figure 1a; the mounting of the polarimeter in the rocket is shown in Figure 1b. In use, the polarimeter is pointed toward the source and rotated about the line of sight. If the incident radiation is polarized, the counting rate in each of the counters will be modulated at a frequency equal to twice the rotation frequency of the polarimeter; the depth and phase of the modulation provide a direct measure of the magnitude and position angle of the polarization vector (see Figure 2a). This mode of operation avoids false indications of polarization that would otherwise arise from differences in the counter sensitivities, amplifier gains, and pulse-height discriminator levels. Clearly, the modulation components of the orthogonal counters must be in antiphase; this fact allows us to discriminate against rapid changes in source strength which might otherwise appear as polarization. The size of the blocks is determined by the mean scattering length in lithium, about 10 cm. The blocks are 12.7 cm deep, sufficient to give a 70% probability of scattering, while the cross section of 25 cm^2 is small enough to avoid multiple scattering. The measured effective area of the polarimeter for unpolarized X-rays is shown in Figure 2b. The limits of sensitivity of the polarimeter are determined at low energies by the photoelectric absorption in the lithium and at high energies by the transparency of the counter gas to hard X-rays.

The response of a single polarimeter module to a beam of 100%-polarized brems-

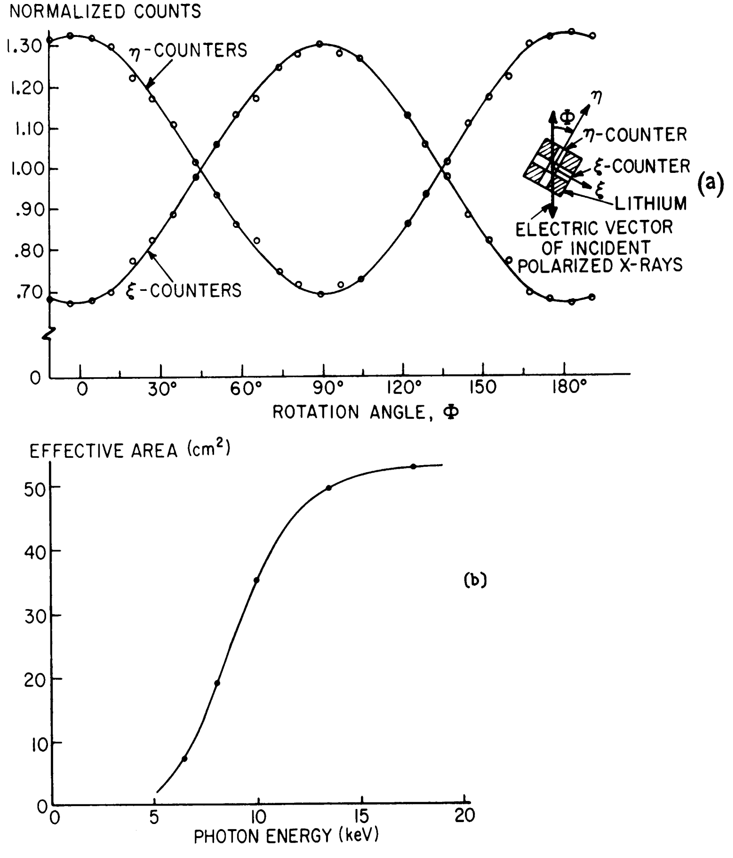

Fig. 2. (a) Variation in the counting rates for each of the orthogonal counters as the polarimeter is rotated with respect to a beam of 100%-polarized X-rays. The counting rates have been normalized to their average values. (b) Variation in the effective area of the polarimeter with photon energy. Note that the geometrical area of the polarimeter is about 900 cm^2.

strahlung X-rays with average energy of 15 keV is shown in Figure 2a. Here are shown the counting rates in each of the two sets of orthogonal counters as a function of the orientation. These rates have been normalized to their average values. As expected, the counts in the two sets of orthogonal counters vary harmonically with angle according to the equations

$$N_\xi = R_0 (1 - M_0 \cos 2\Phi),$$
$$N_\eta = R_0 (1 + M_0 \cos 2\Phi).$$

Here R_0 is the average counting rate, and M_0 is the depth of modulation for 100%-polarized X-rays; the axes ξ and η and the rotation angle Φ are defined in Figure 2a. Because each of the detectors subtends a large solid angle, the modulation depth M_0 has a value of only 31.6% for a 100%-polarized beam. Any attempt to increase the depth of modulation by decreasing the solid angle of the counters would reduce the efficiency and increase the minimum detectable polarization.

There are additional possible sources of systematic errors that must be considered. If the instrument were not pointed directly at the X-ray source, orthogonal detectors would not be equally illuminated, and a false indication of polarization would be obtained. Laboratory experiments showed that the instrument axis had to be pointed within 3° of the source to keep this effect small. To check the proper orientation of the rocket, an optical star sensor was used to determine the rocket orientation and a collimated forward-looking X-ray detector was built into the instrument. Systematic errors could be contributed by anisotropies in the background counts arising from cosmic rays and albedo gamma rays from the earth's atmosphere. Anisotropy of this radiation could result in orientation dependence of the background counting rate. A measurement of the background counting rate was carried out on a prototype instrument flown to a height of 95000 ft in a balloon. The instrument was rotated about a vertical axis, and a search was made for apparent polarization effects that might arise from the known east-west anisotropy of the cosmic-ray protons. No effect large enough to affect the present results was observed.

The payload is illustrated in Figure 1b. After the nose cone is ejected, X-rays enter the scattering blocks through a collimator which gives a clear view up to 3° from the axis and is totally opaque for angles greater than about 12°. This collimator prevents illumination by other X-ray sources and severely limits the signal from the isotropic background. The counter-scatterer assembly is surrounded by an anticoincidence shield of scintillating plastic viewed by a 3-in. photomultiplier tube. The forward-looking X-ray detector is located in the corner of the main polarimeter. Charge-sensitive preamplifiers are mounted on each counter forming the lower part of the main collimator. In the main electronic processing unit, the heights of the pulses from each amplifier, which are not vetoed by the plastic scintillator, are analyzed separately into four bins, corresponding to detected photon energies of 5.5–11 keV, 11–16.5 keV, 16.5–22 keV, and above 22 keV. Four scalers for each channel accumulate the counts in each energy bin and are sampled every 12 msec by the telemetry system. A detailed description of the instrument will be given elsewhere.

Cosmic-ray background poses the greatest limitation in the detection of X-ray polarization in weak sources such as the Crab nebula. Although the polarimeter is surrounded by a plastic anticoincidence shield to veto energetic charged particles, leakage due to solid angle factors and the materialization of neutrals inside the shield lead to a background rate of 0.01 counts/cm^2 sec keV in each of the proportional counters measured above the atmosphere (Angel *et al.*, 1969). With recent data on the X-ray flux from the Crab and the measured spectral response of the instrument, a background-to-signal ratio of 4:1 was estimated. This would have imposed severe statistical limitations on the experiment. Substantial additional background suppression was accomplished by using rise-time discrimination which makes use of the different pulse shapes caused by charged particles and X-rays. Laboratory tests indicated that the background-to-signal ratio could be reduced to 1.2:1.

The aspect of the rocket during the flight was controlled with a system of gyros and was monitored by the forward-viewing X-ray detector and star sensor. During the 4-min data-acquisition period, the polarimeter remained pointed to within 1.5° of the source and rotated around the line of sight at 6.4°/sec. The energy levels of the pulse height discriminators were set using X-ray sources, and the calibration was checked 3 h prior to launch. The number of counts observed are listed in Table I. During the 4 min of flight while data from the source were being taken, the anticoincidence rate was 1300/sec, leading to a negligible correction for dead time. The background counts were obtained by analyzing the data after the nose cone was ejected but before the instrument was pointed at the target and again after active control was lost until the Pfotzer cosmic-ray maximum was approached on re-entry; 53 sec of background data were obtained. The signal counting rate closely conformed to the predictions based on previous data.

TABLE I

Source data: 240 sec

Bin	Energy range (keV)	X-ray counts	Counts/counter-sec
1	5.5 – 11	2499 ± 171	0.651 ± 0.045
2	11. – 16.5	2996 ± 186	0.782 ± 0.0485
3	16.5 – 22	1771 ± 176	0.461 ± 0.046

Background data: 53 sec

Bin	Counts	Counts/counter-sec
1	1095	1.284 ± 0.039
2	1303	1.5279 ± 0.042
3	1189	1.3942 ± 0.040

The data were analyzed for polarization by looking for modulation in the counting rate in phase with the roll of the rocket. The data for each counter were fitted by least squares to the function

$$R(t) = S_0 (1 + M_1 \cos 2\omega t + M_2 \sin 2\omega t) \tag{1}$$

where $R(t)$ represents the observed counting rate, S_0 the background and the average X-ray intensity, and M_1 and M_2 are the modulation coefficients, related to the total modulation by $M = (M_1^2 + M_2^2)^{1/2}$. The phase of the modulation Ψ is defined by $\Psi = \frac{1}{2} \tan^{-1}(M_2/M_1)$. The modulation components for the signal-plus-background data were calculated for each energy bin of each counter, or a total of 64 pairs of numbers. The standard deviation of each component was also calculated, using the definition of variance for a single 1-sec sample of data and propagating this uncertainty through the equations of least squares.

The mean background rates were subtracted from the mean signal-plus-background rates S_0 to obtain a net mean signal rate S_0' for each counter and bin. The signal modulation components M_1' and M_2' were then calculated using the net rates, resulting again in 64 pairs of components. The standard deviations were also combined in the appropriate way. The 16 proportional counters are oriented in two orthogonal directions designated X and Y, forming two separate polarimeters. Modulation components for the eight counters in the X polarimeter were then weighted by their standard deviations and added, and the same procedure was followed for the Y counters. The weighted sums were computed for the lower three bins, and the fourth bin, corresponding to photons above 22 keV, was neglected as it contained virtually no signal. Since the X and Y counters are orthogonal, modulation in their counting rates due to signal polarization must display appropriate phase differences. The X and Y modulation components were then added by taking this phase difference into account. The resultant modulation components for the X-ray signal detected in the three bins, with their standard deviations, are listed in Table II, together with the weighted sum of the three bins. The components have been referenced to the celestial sphere using magnetometer aspect data, so that M_1' and M_2' now correspond to the same coordinate system in which the Stokes parameters are expressed. A striking feature of these results is the lack of a common direction among the modulations calculated for the three bins. Although the results for each bin when taken separately are suggestive of a nonzero modulation, their sum is consistent with a null result.

A check of the validity of the calculation procedure was accomplished by a Monte Carlo simulation of the experiment. Twenty-two thousand counts randomly distributed over 240 sec were generated and analyzed for modulation. The procedure was repeated 100 times. The standard deviations obtained by Monte Carlo simulation correspond closely to those achieved by calculation from the flight data, and its modulation is consistent with that of the sets of random data. There is a probability of obtaining a nonzero value of the modulation from purely random data since each of the components is statistically independent. The probability of obtaining modulation M, is given by

$$W(M)\,\mathrm{d}M = \frac{MN}{2} \exp - \frac{M^2 N}{4}\,\mathrm{d}M \tag{2}$$

https://doi.org/10.1017/S0074180900007208 Published online by Cambridge University Press

TABLE II

Modulation components and normalized Stokes parameters

Bin	Energy range (keV)	M'_1	M'_2	q	u	Polarization P	Position angle θ (degrees)
1	5.5 – 11.0	0.082 ± 0.048	0.043 ± 0.047	0.262 ± 0.152	0.138 ± 0.150	0.30 ± 0.15	14
2	11.0 – 16.5	-0.014 ± 0.045	-0.032 ± 0.045	-0.046 ± 0.143	-0.262 ± 0.143	0.27 ± 0.14	130
3	16.5 – 22.0	-0.019 ± 0.069	0.010 ± 0.067	-0.061 ± 0.218	0.032 ± 0.216	0.07 ± 0.22	76
1 + 2 + 3	5.5 – 22.0	0.023 ± 0.030	-0.016 ± 0.029	0.072 ± 0.095	-0.050 ± 0.095	0.088 ± 0.095	163

with a mean value

$$\langle M \rangle = (\pi/N)^{1/2}.$$

Here N is the total number of counts obtained in the observation.

The data were analyzed for modulation at a range of frequencies close to the roll rate to examine the correlation between the signal modulation and frequency. If the apparent modulation is due to polarization, then the modulation should be a maximum at twice the roll rate; but if the modulation is due to a statistical fluctuation, the two quantities will be uncorrelated. The calculation was performed at rocket rotation periods ranging from 45 to 75 sec at intervals of 0.75 sec, and also at the true rotation period of 56 sec. Monte Carlo data were generated with varying amounts of modulation at the roll frequency, and subjected to the same analysis. The results, graphed as modulation versus period, are shown in Figure 3. Monte Carlo cases with less than

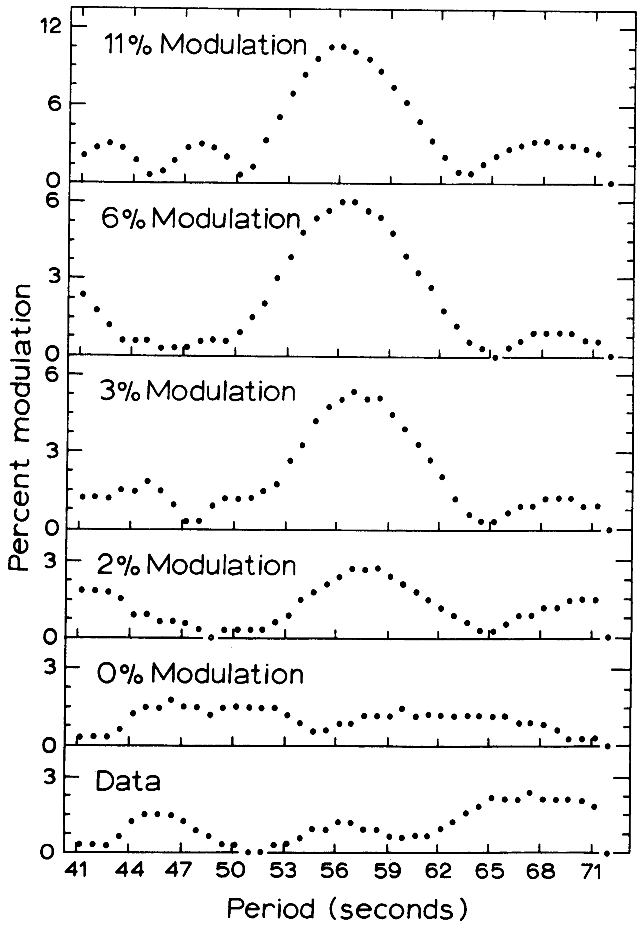

Fig. 3. Percent modulation as a function of rotation frequency for flight data and Monte Carlo trials. Varying amounts of modulation with a period of 56 sec have been introduced in the Monte Carlo trials.

https://doi.org/10.1017/S0074180900007208 Published online by Cambridge University Press

3% modulation are indistinguishable from purely random data. The maximum at the roll period begins to appear at 4% modulation, but is clearly missing in the real data.

Possible instrumental effects leading to cancellation of the source modulation were explored. Modulation in the background rate was assumed to be zero, but, if not, could add in antiphase to the signal modulation leaving a null result. Data from a balloon flight in 1967 and a rocket flight in 1968, using similar versions of the polarimeter, showed no evidence for background modulation. In the first flight the polarimeter was pointed toward the zenith, while in the second it was inclined at an angle of 45°. In the current flight, the instrument was aimed at 14° from vertical. Anisotropy in the albedo flux from the earth's atmosphere must be eliminated since neither of the earlier flights offer evidence for existence of this effect. An anisotropy in the primary cosmic-ray flux, such as the east-west effect, could manifest itself as spurious modulation. A search for this effect was made by analyzing the fourth bin ($E > 22$ keV) data for modulation. The events in the channel were entirely due to the cosmic-ray background. A very small modulation, $M = 0.007 \pm 0.0075$, consistent with zero, was discovered. The effectiveness of the polarimeter background suppression methods was tested using a monoenergetic and monodirectional charged-particle beam generated by the Princeton-Penn accelerator (PPA). Comprised of 1 BeV/c protons, the PPA beam was incident on the side of the polarimeter perpendicular to its longitudinal axis, and the counting rates at various azimuthal orientations monitored. No effects which would lead to spurious evidence for polarization were encountered.

If a cosmic-ray-induced modulation existed and were energy dependent, then the dispersion in direction of the modulations for the three bins might be explained. However, if cosmic-ray primary protons are interacting, they must be entering the polarimeter through the front, or they would be detected and vetoed by the anti-coincidence shield. This limits their trajectories to angles of 60° or less with respect to the line of sight of the instrument. The magnetic rigidity of the earth at 30°N latitude is substantial, and truncates the proton spectrum at about 2 BeV. Such minimum ionizing particles, passing through the three atmospheres of xenon, would deposit at least 40 keV in one orientation of a detector, and twice this in the other. Only very unusual paths, such as through the corners of the counters, would result in the deposition of a small enough energy for a primary cosmic ray to be recorded in one of the three signal bins.

Conclusions regarding the maximum likely polarization of the X-ray flux of the Crab nebula can be drawn from these results. The degree of polarization P is related to a detected modulation M by the equation

$$P = \mu M ,$$

where μ has been measured to be 3.16. The probability of measuring a polarization of 10% or less, with a 1σ uncertainty of 9% in each of the components has been calculated for various true polarizations P. The probability of obtaining our result, or smaller, given a true source polarization of 27%, is less than 1%. This argument establishes an upper limit of 27% on the X-ray polarization of the nebula with a 99% confidence level. There is a 95% probability that the source polarization is not greater than 20%. The position angle of polarization vector obtained is 163°, which compares favorably with that of the radio and optical results, as can be seen in Figure 4. Although suggestive, this apparent correlation cannot be rigorously interpreted as evidence for a positive result, because the uncertainty in the polarization components is sufficiently large to include all angles in the 1σ circle of uncertainty.

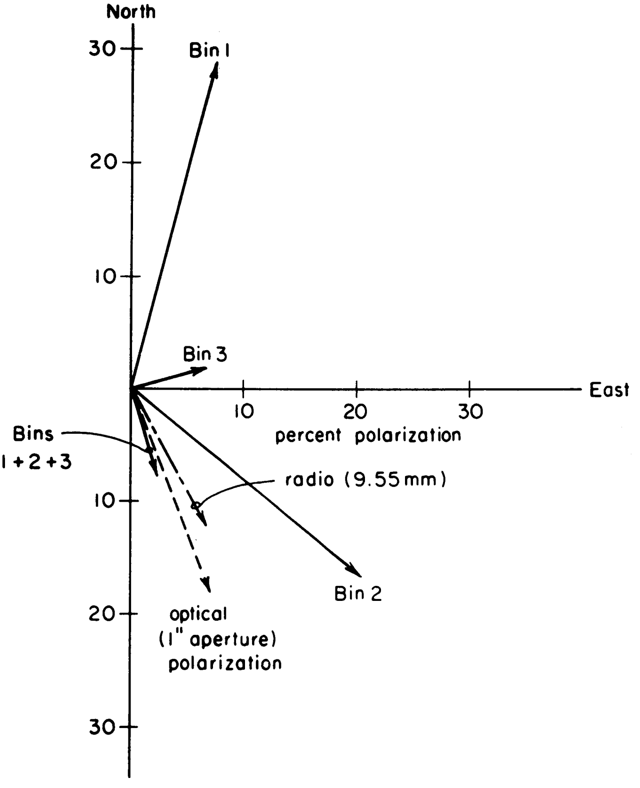

Fig. 4. The polarization vectors shown are in terms of celestial coordinates. The numbers beside the vectors correspond to the energy bin.

In summary, our results can best be interpreted as setting an upper limit of 27% on the polarization of the X-ray emission of Taurus X-1 with a 99% confidence level. The present result does not serve to distinguish between synchrotron and other processes suggested for X-ray production in the Crab nebula.

References

Angel, J. R. P., Novick, R., Vanden Bout, P., and Wolff, R.: 1969, *Phys. Rev. Letters* **22**, 861.
Bowyer, S., Byram, E. T., Chubb, T. A., and Friedman, H.: 1964, *Science* **146**, 912.
Hobbs, R. W.: 1968, *Astrophys. J.* **153**, 1001.

Oda, M., Brandt, H., Garmire, G., Spada, G., Sreekantan, B. V., Gursky, H., Giacconi, R., Gorenstein, P., and Waters, J. R.: 1967, *Astrophys. J.* **148**, L5.
Oort, J. H. and Walraven, Th.: 1956, *Bull. Astron. Inst. Neth.* **12**, 285.
Sartori, L. and Morrison, P.: 1967, *Astrophys. J.* **150**, 385.
Vashakidze, M. A.: 1954, A. Ts., No. 147.
Wolff, R. S., Angel, J. R. P., Novick, R., and Vanden Bout, P.: 1970, *Astrophys. J.* **160**, L21.
Woltjer, L.: 1964, *Astrophys. J.* **140**, 1309.

Discussion

N. Visvanathan: Does the 19% polarization which you expect include an allowance for measuring efficiency?

R. Novick: Yes.

N. Visvanathan: The optical polarization varies across the Crab Nebula. Near the pulsar it is only 4%.

R. Novick: The signal which we are measuring is the integrated emission. Our limit suggests that if the X-radiation is synchrotron emission it is not coming from a region of very homogeneous field.